

# GENERALIZED GEERTSMA SOLUTION FOR ISOTROPIC LAYERED MEDIUM

Joonsang Park<sup>1\*</sup>, Ola Eiken<sup>2</sup>, Tore I. Bjørnarå<sup>1</sup>, Bahman Bohloli<sup>1</sup>

<sup>1</sup> Norwegian Geotechnical Institute (NGI), Oslo, Norway

<sup>2</sup> Quad Geometrics, Trondheim, Norway

\* Corresponding author e-mail: [jp@ngi.no](mailto:jp@ngi.no)

## Abstract

We report a generalized Geertsma solution with which we can calculate the surface deformation from a subsurface made of an arbitrary number of isotropic homogeneous layers and a thick reservoir at any depth. We validate the generalized Geertsma solution by solving simple numerical examples and comparing the results with a reference finite-element solution. Then, we apply the generalized Geertsma solution to more realistic subsurface models to study the effect of subsurface layering on surface deformation and the impact of acquisition-processing accuracy on inverted reservoir pressure. The modelling demonstrates the surface deformation (both magnitude and shape) is most influenced by the reservoir stiffness. Finally, the inversion exercise demonstrates that for the case of In Salah-inspired synthetic model, 3% noise resulting from data acquisition-processing error may introduce 15% deviation in the inverted pressure compared to the true reservoir pressure.

**Keywords:** *surface heaving, Geertsma solution, layered subsurface, CO<sub>2</sub> injection*

## 1. Introduction

Carbon capture and storage (CCS) is a promising technology that can significantly reduce the greenhouse gas emission from large-scale industrial point sources to the atmosphere. At the same time, there are several challenges to resolve. One urgent challenge is pressure control in the subsurface during CO<sub>2</sub> injection so that we can secure the integrity of the storage complex as well as optimize the injection rate. The Sleipner CO<sub>2</sub> storage is an example where there is no pressure build-up observed at the wellhead during more than 20 years of injection thanks to the good reservoir quality of the Utsira sand in the North Sea (Furre et al, 2015). On the other hand, the In Salah CO<sub>2</sub> storage project has experienced pressure increase to near fracture pressure in the injection well (Bohloli et al, 2018). Associated surface uplift was clearly detected with InSAR and showed how the reservoir pressure build-up was distributed in the subsurface, even delineating the temporal evolution of the footprint of a vertical fault near the KB502 injector (Bohloli et al, 2018, Bjørnarå et al, 2018).

Such precise surface deformation data is a direct response to the spatial and temporal distribution of pressure changes in the subsurface. Therefore, it is desired to have a good framework of interpreting and inverting the surface deformation in order to precisely map pressure changes and furthermore characterize geomechanical and hydraulic properties (Vasco et al, 2017). To achieve this, we need to have an accurate and fast engine to calculate surface deformation for a given pressure disturbance and a given subsurface model. Geertsma (1973) derived a closed-form solution that can calculate very quickly such surface deformations, assuming the subsurface is a homogeneous half-space. In addition, the Geertsma solution assumes the thickness of the pressure-disturbed

reservoir is much smaller than the depth of the reservoir. Mehrabian and Abousleiman (2015) overcame the homogeneous half-space limitation by modelling up to three layers using the same mechanical properties in the overburden and underburden. Here we generalize the framework in Mehrabian and Abousleiman (2015) so that we can handle: 1) arbitrary number of isotropic homogeneous layers, and 2) thick reservoir at any depth (Figure 1). We also seek to correct a few critical typographical errors in Mehrabian and Abousleiman (2015). Then, we validate the generalized Geertsma solution for the isotropic layered half space (ISO-GGS or just GGS) by solving simple numerical examples and by comparing with a reference finite-element-based solution. Finally, we apply the generalized Geertsma solution to more realistic subsurface models (inspired by an In Salah model) to study: 1) the effect of layered models on predicted surface deformation, and 2) the impact of acquisition-processing errors of surface deformation on reservoir pressure inverted with the help of such models.

## 2. Generalized Geertsma solution (GGS) for isotropic layered subsurface

Mehrabian and Abousleiman (2015) present a mathematical framework and derive a fully closed-form analytical solutions for stress tensor and deformation vector outside and inside an isotropic homogeneous reservoir layer embedded within another isotropic homogeneous half-space of dissimilar mechanical properties. In the closed-form solution, the reservoir layer should be quite thin compared to the reservoir depth and is subjected to axisymmetric constant pore pressure disturbance with finite radius. Although the final result plots are accurately given in Mehrabian and Abousleiman (2015), it is found during the current study

that there are critical typos in the description of the mathematical framework. The errors are discovered and corrected by following the linear elasticity framework in Park and Kaynia (2018). The kernels in Eqs 7-8 and 12-13 in Mehrabian and Abousleiman (2015) should have been written:

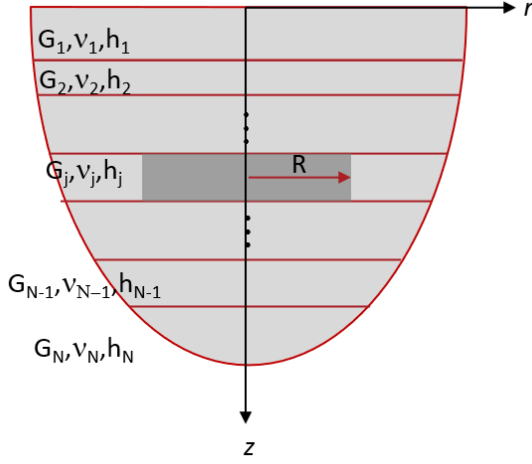


Figure 1: Isotropic subsurface model consisting of  $N$  layers and subjected to fluid-induced pore pressure (shaded) of radius  $R$  in a  $j$ -th layer. Note  $G$ ,  $\nu$  and  $h$  are shear modulus, Poisson's ratio and thickness of each layer. Axi-symmetric coordinates  $(r, z)$  are used.

$$U_1 = \frac{c_m P}{k} + az(Ae^{kz} - Be^{-kz}) + Ce^{kz} + De^{-kz}$$

$$U_3 = \left(\frac{a+1}{k} - az\right)Ae^{kz} - \left(\frac{a+1}{k} + az\right)Be^{-kz} - Ce^{kz} + De^{-kz}$$

$$S_{rz} = 2G \left[ \left(akz - \frac{1}{2}\right)Ae^{kz} + \left(akz + \frac{1}{2}\right)Be^{-kz} + kCe^{kz} - kDe^{-kz} \right]$$

$$S_{zz} = 2G \left[ \left(1 - akz + \frac{\nu}{1-2\nu}\right)Ae^{kz} + \left(1 + akz + \frac{\nu}{1-2\nu}\right)Be^{-kz} - kCe^{kz} - kDe^{-kz} - c_m P \right]$$

where  $a = 1/2(1 - 2\nu)$ ,  $c_m = \alpha(1 - 2\nu)/2G\nu$ ;  $\nu$  and  $G$  are Poisson's ratio and shear modulus;  $k$  is the wavenumber for the associated Hankel transform;  $z$  is the depth-direction coordinate;  $P=R/kJ_1(kR)$  is magnitude of pore pressure disturbance in  $k$  domain with  $R$  and  $J_1$  being the radius of the constant pore pressure disturbance and the 1<sup>st</sup>-order Bessel function;  $A$ ,  $B$ ,  $C$  and  $D$  are unknown coefficients to be determined based on the boundary conditions in the layered subsurface i.e. continuity conditions of horizontal-vertical displacements ( $U_1$  and  $U_3$ ) and shear-normal stresses ( $S_{rz}$  and  $S_{zz}$ ) at each interface as described in Mehrabian and Abousleiman (2015). Performing the associated Hankel transformation, we can calculate the displacements and stresses at any point in a given isotropic multilayered subsurface subjected to a pore pressure change applied at any layer.

## 2.1 Validation

We validate the corrected expressions against a finite element method solution. We run a numerical example of

three layers and compare with the commercial code COMSOL Multiphysics™. Table 1 shows the material properties and thicknesses of the layered subsurface. We consider three models by varying the ratio ( $\mu$ ) of shear moduli between Layer 2 and Layers 1 & 3 as shown in Table 1. Layer 2 is subjected to a 10 MPa pore pressure disturbance of cylinder shape with radius of 500 m. The results of the vertical displacement at the top surface (subsidence) are shown in Figure 2. It can be seen that the two solutions obtained by the generalized Geertsma (ISO-GGS) and FE solutions (solid lines and circles, respectively) are in good agreement. Additionally, we can see the significant effects of multilayers (in both magnitude and shape of surface deformation) by looking at the differences between the layered models (models 1, 3) and the homogeneous model (model 2).

Table 1: Material properties for the validation models. Poisson's ratio is 0.25 for all the layers.

layer	thickness [m]	shear modulus ( $G$ ) [GPa]		
		model 1	model 2	model 3
1	1300	0.5	1.0	2.0
2	200	1.0	1.0	1.0
3	$\infty$	0.5	1.0	2.0

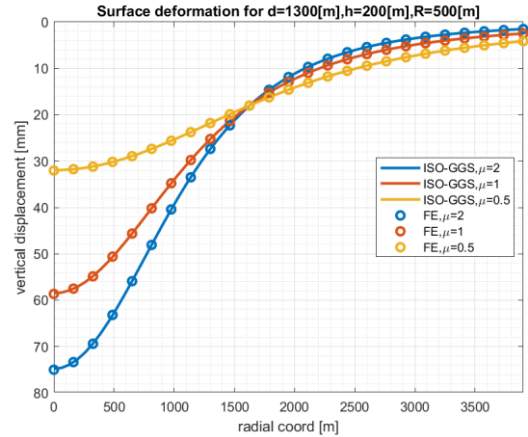


Figure 2: Comparison of the generalized Geertsma solution for isotropic subsurface (ISO-GGS, solid lines) and the finite element solution (FE, circles) for three different values for  $\mu (=G_{1,3}/G_2) = 0.5, 1.0$  and  $2.0$ . Note that the vertical axis in the plot has the positive downward convention.

## 3. Synthetic data study via In Salah model

### 3.1. Effect of layer stiffness on surface deformation

To increase our understanding of the relationship between the surface deformation and the layer stiffness, we solve a series of four numerical examples by tuning layer stiffnesses (Figure 3). The reference model is taken from Bjørnarå et al (2018) for the In Salah CO<sub>2</sub> storage project. The other models are made by softening the Young's moduli by 25% in either the overburden layers, the reservoir layer or the underburden, respectively. Figure 4 shows the comparison of the four models in terms of vertical displacement at the top surface.

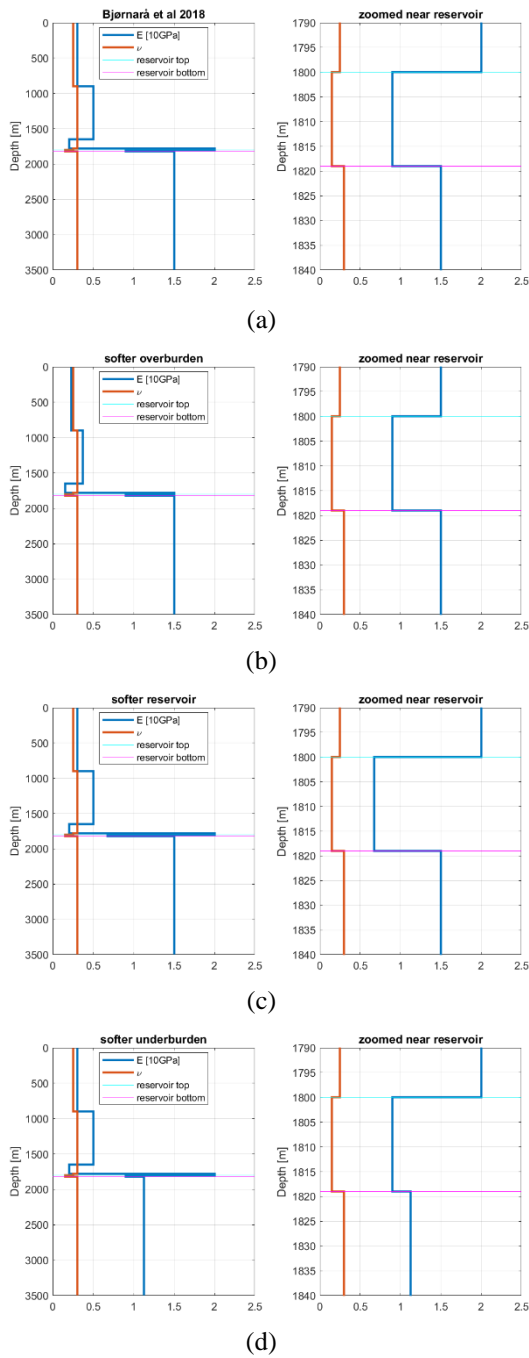


Figure 3: Four subsurface layer models taken from Bjørnå et al (2018): (a) reference model; (b) 25% softer overburden; (c) 25% softer reservoir; (d) 25% softer underburden.

Not surprisingly, the surface vertical displacement is strongly dependent on the layer stiffness. It can also be seen in this analysis that the stiffness of the reservoir (where the pore pressure disturbance is applied) has the most influence on the magnitude of vertical displacement (yellow curve in Figure 4), while the stiffness of the overburden has the least influence. The result of the softer overburden model (red curve) is very close to the reference model in both magnitude and shape. However, the softer underburden (purple curve) makes the top surface heave smaller compared to the reference model (blue curve) for  $r < 2500\text{m}$ , but (slightly) larger for  $r > 2500\text{m}$ . When the underburden becomes stiffer instead, it is expected that the surface heave becomes

larger for  $r < 2500\text{m}$  and smaller for  $r > 2500\text{m}$ . We can see that the surface height change (in both magnitude and shape) is more sensitive to the stiffness of the underburden than the overburden. All these observations provide us with good insights on the correlation between the surface deformation and the subsurface layering, which is challenging for interpretation and inversion of the surface deformation measured by e.g. InSAR (e.g. Bohloli et al, 2018) or seabed pressure (Eiken et al, 2008).

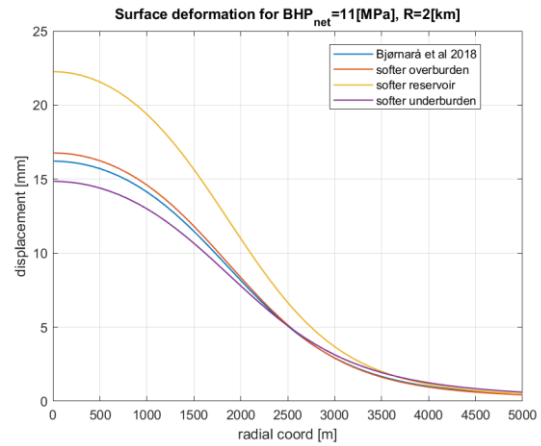


Figure 4: Comparison of top surface vertical displacements for the four subsurface models shown in Figure 3. Note that the vertical axis in the plot has the positive upward convention.

### 3.2. Impact of acquisition-processing accuracy on inverted reservoir pressure

High accuracy in data is generally important for characterization and monitoring of the subsurface. In particular, the surface height changes estimated from processed onshore InSAR and seabed pressure requires precision of mm-scale to be detectable, which is challenging at the field scale. In this subsection, we demonstrate the impact of the accuracy of surface deformation obtained through the acquisition-processing on the inversion result for reservoir pressure on synthetic data. We model surface uplift from the subsurface model of Figure 3a by using the generalized Geertsma solution, and assuming the reservoir pressure spatial distribution as shown in Figure 5a. To create the synthetic solution, 3% random noise is added to the calculated heave. Finally, we invert for the reservoir pressure (Figure 5b) and compare it to the synthetic reservoir pressure (Figure 5a), which was input to the forward modelling and inversion exercise. The inversion problem considered here is based on a linear superposition relationship between surface deformation and pressure change, and the detail can be found in Park et al. (2021). Figure 5c shows the difference between the synthetic and inverted reservoir pressure. The 3% noise that was added to create the synthetic solution causes absolute errors in the inverted pressure up to 1.6 MPa, which is more than 15% deviation at the locations with maximum pressure changes. Therefore, it is important to reduce the uncertainty in the surface deformation data, involving

technical improvements in both acquisition and processing of InSAR and seabed data.

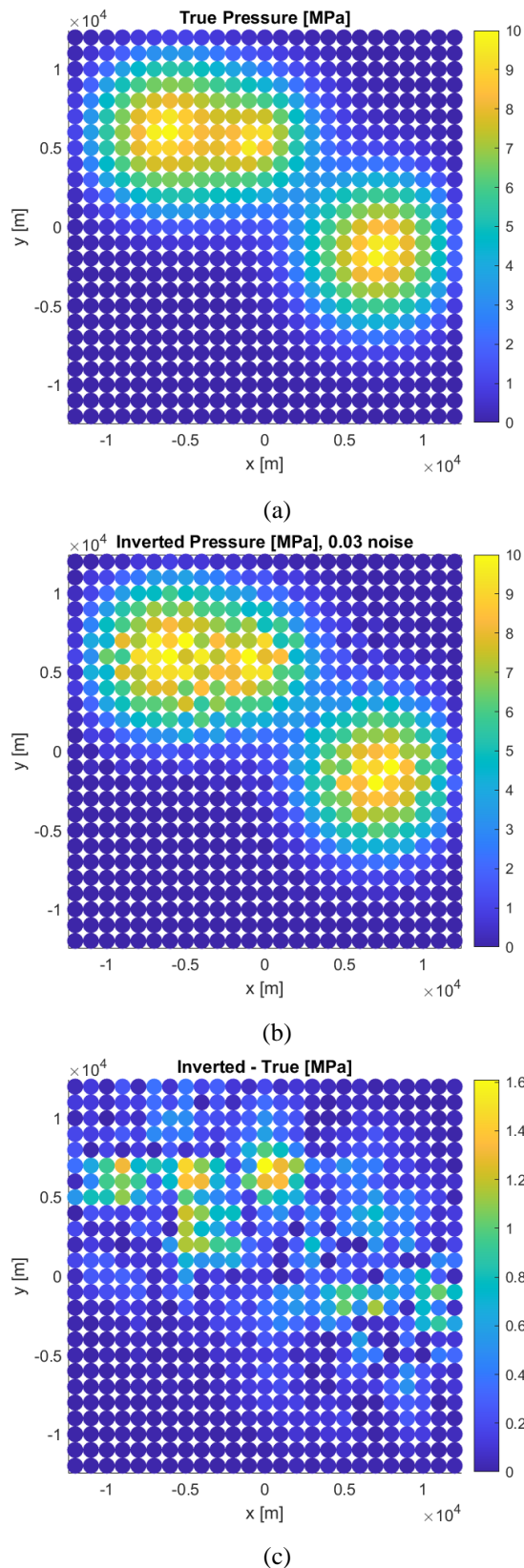


Figure 5: (a) Reservoir pressure change distribution input to the synthetic data calculation, inspired by Bjørnarå et al. (2018); note that from left to right, three pressure anomalies are related to the three injection wells of KB503, KB502 and KB501, respectively); (b) inverted reservoir pressure distribution; (c) difference between "true" and inverted reservoir pressures.

## 4. Summary and conclusion

In the current study, we have described the generalized Geertsma solution (GGS) that can handle arbitrary number, depth and thickness of isotropic homogeneous layers. The solution is validated by comparing the analytical solution to a numerical solution. We have applied the GGS to various subsurface models to study the effect of subsurface layering on surface deformation and the impact of acquisition-processing accuracy on inverted reservoir pressure. It is shown that, for the tested case-study inspired by the In Salah CO<sub>2</sub> storage project, the surface deformation is particularly dependent on the mechanical properties of the reservoir. Finally, the inversion exercise has demonstrated that 3% noise due to acquisition-processing error may introduce up to 15% error in the inverted pressure.

## Acknowledgements

The study is supported jointly by 1) SENSE (Assuring integrity of CO<sub>2</sub> storage sites through ground surface monitoring, CLIMIT Demo Project No. 299664, ACT2-EC Project no. 691712) and 2) SHAPE (Seafloor height from aqua pressure for offshore CO<sub>2</sub> storage, CLIMIT Demo Project No. 620080). Equinor and Quad Geometrics are the industry partners.

## References

- [1] Bohlooli, B., Bjørnarå, T.I., Park, J., Rucci, A. (2018). Can surface uplift be used as a tool for monitoring reservoir performance? A case study from In Salah, Algeria, *International Journal of Greenhouse Gas Control*, 76, 200-207.
- [2] Bjørnarå, T. I., Bohlooli, B., Park, J. (2018). Field data analysis and hydromechanical modeling of CO<sub>2</sub> storage at In Salah, Algeria. *International Journal of Greenhouse Gas Control*, 79, 61-72.
- [3] Eiken, O., Stenvold, T., Zumberge, M.A., Alnes H., Sasagawa G. (2008). Gravimetric monitoring of gas production from the Troll field. *Geophysics* 73(6) WA 149 - WA 154.
- [4] Furre, A.K., Kiær, A., Eiken, O. (2015). CO<sub>2</sub>-induced seismic time shift at Sleipner, *Interpretation*, 3(3), SS23-35.
- [5] Geertsma, J. (1973). A basic theory of subsidence due to reservoir compaction: the homogeneous case. *Trans. R. Dutch Soc. Geol. Min. Eng.* 28, 43-62.
- [6] Mehrabian, A., Abousleiman, Y.N. (2015). Geertsma's subsidence solution extended to layered stratigraphy, *Journal of Petroleum Science and Engineering* 130, 68-76.
- [7] Park, J., Kaynia, A.M. (2018). Stiffness matrices for fluid and anisotropic soil layers with applications in soil dynamics, *Soil Dynamics and Earthquake Engineering*, 115, 169-182.
- [8] Park, J., Bjørnarå, T.I., Bohlooli, B. An Analytical Solution for Pressure-Induced Deformation of Anisotropic Multilayered Subsurface. *Geosciences* 2021, 11, 180. <https://doi.org/10.3390>.
- [9] Vasco, D.W., Harness, P., Pride, S., Hoversten, M. (2017). Estimating fluid-induced stress change from observed deformation, *Geophysical Journal International*, 208(3), 1623-1642.